

BIODIESEL PRODUCTION FROM PALM STEARIN PROCESS OPTIMISATION USING RESPONSE SURFACE METHODOLOGY (RSM)

P GOWTHAM^{1*}; K PITCHANDI² and V MANIENIYAN¹

ABSTRACT

The purpose of this study is to optimise biodiesel production from palm stearin using the Box-Behnken design in response surface methodology (RSM) for three key process parameters: Methanol volume, catalyst concentration and reaction time. The methanol (A) was fixed at three levels: -1, 0, and +1, corresponding to 200, 225 and 250 mL, respectively; the catalyst (B) concentration was varied between 8, 10, and 12 g; and the reaction time (C) ranged from 45-90 min. The experiments were conducted and analysed using Design Expert software (version 13) to maximise biodiesel yield. The highest yield of palm stearin methyl ester (910 mL, 89.25% yield) was achieved with 225 mL methanol, 10 g catalyst and a reaction time of 60 min. The optimised model predicted a yield of 913.4 mL, demonstrating strong agreement with experimental results. This study is significant in promoting more sustainable biodiesel production by improving efficiency and reducing both operational costs and environmental impact. By optimising process parameters, this work addresses the need for cost-effective renewable fuel alternatives, contributing to the long-term commercial viability of biodiesel in the energy market.

Keywords: biodiesel, Box-Behnken Design, catalyst, RSM, transesterification.

Received: 3 January 2024; **Accepted:** 22 November 2024; **Published online:** 20 February 2025.

INTRODUCTION

To address energy security concerns and reduce the environmental impact of fossil fuels, the search for sustainable and renewable energy sources has become crucial. Biodiesel, derived from animal fats and vegetable oils, presents a viable alternative to conventional fossil fuels by lowering greenhouse gas emissions and reducing reliance on non-renewable resources. Palm stearin, a product of palm oil fractionation with high saturated fat content, has been identified as a potential feedstock for biodiesel production. Sustainable palm oil practices are also being promoted to encourage the use of this renewable resource.

Vegetable oils and fats often contain impurities like gums, free fatty acids (FFA), and metal components that must be removed to improve oil quality (Adepoju *et al.*, 2022). Acid oil, a by-product of oil refining, is a low-cost alternative to refined oils and is suitable for biodiesel production when impurities are reduced (Muthuswamy & Veerasigamani, 2020).

Biodiesel produced from waste oil can match the quality of petroleum diesel, and palm stearin is a favourable feedstock for its synthesis. Extracted from the oil palm tree (*Elaeis guineensis*), particularly in Southeast Asia, palm stearin offers high yields at a lower cost than other feedstocks. Its composition, rich in saturated fatty acids, enhances the transesterification process, making it suitable for biodiesel production.

Edible palm stearin, with its high saturated fat content and solidification properties, was chosen over alternatives like palm kernel oil (PKO), palm oil mill effluent (POME) and palm fatty acid distillate (PFAD). Palm stearin's saturated fats, especially palmitic acid, provide higher cetane numbers,

¹ Department of Mechanical Engineering, Government College of Engineering Srirangam, Tamil Nadu, India.

² Department of Mechanical Engineering, Sri Venkateswara College of Engineering, Tamil Nadu, India.

* Corresponding author e-mail: gowthamvortex@gmail.com

improving combustion and ignition. Its solid fraction enhances cold flow properties, lowering the cloud point and improving performance in colder climates (Hazrat *et al.*, 2020). In contrast, PKO's lower saturated fat content may require additional processing to meet biodiesel standards. POME and PFAD, while potential feedstocks, contain impurities and FFA that complicate biodiesel production, raising costs (Zahan & Kano, 2018).

Biodiesel made from palm stearin, a by-product of the palm oil industry, offers significant environmental advantages, such as reducing greenhouse gas emissions and contributing to waste management by converting a low-value material into a renewable energy source. Additionally, palm stearin is a cost-effective feedstock compared to virgin oils, lowering the overall production costs and improving the market competitiveness of biodiesel. These factors not only make biodiesel from palm stearin environmentally sustainable but also economically viable, aligning with global efforts to reduce carbon emissions and promote renewable energy.

Jatropha oil may yield higher oil content, but palm stearin, as a by-product of palm oil processing, offers a more cost-effective and sustainable alternative. Waste oils, although potentially cheaper, often require more complex processing due to contamination and impurities.

Transesterification is a chemical process used in biodiesel production to convert vegetable oils, used frying oil and animal fats into biodiesel and glycerol. This reaction involves the use of an alcohol, typically ethanol or methanol, in the presence of a catalyst such as potassium hydroxide (KOH) or sodium hydroxide (NaOH), to produce biodiesel (Rajali *et al.*, 2022). Upon completion of the transesterification process, the biodiesel can either be used alone or blended with petroleum diesel in various proportions. Single-stage processes commonly use alkali-based catalysts, while two-stage methods may incorporate both alkali and acid catalysts.

Biodiesel exhibits physical properties similar to petroleum diesel, making it suitable for compression ignition (CI) engines without significant modifications (Sonachalam *et al.*, 2020). It can be used as a standalone fuel or blended with diesel in mixes such as B5 or B20, providing benefits like a higher cetane number, better combustion and reduced emissions of particulate matter and carbon monoxide (Ranjan *et al.*, 2022). However, biodiesel has slightly less energy content than petroleum diesel, potentially leading to lower fuel efficiency (Deivajothi *et al.*, 2018) and tends to produce higher nitrogen oxide (NOx) emissions, which can contribute to smog formation (Razak *et al.*, 2021). These challenges can be mitigated with technologies like selective catalytic reduction (SCR) systems.

Using palm stearin for biodiesel production offers environmental advantages by reducing waste and promoting a circular economy, as palm stearin is a by-product of palm oil processing (Bustamam *et al.*, 2022). Biodiesel derived from palm stearin also exhibits favourable combustion properties, including lower greenhouse gas emissions compared to traditional diesel fuels. These properties make palm stearin a promising feedstock for biodiesel synthesis, contributing to sustainable energy solutions.

KOH is widely used as a catalyst in biodiesel production due to its high reactivity, cost-effectiveness, and established industrial use. KOH efficiently catalyses the transesterification of triglycerides, accelerating reaction kinetics and reducing by-products, which simplifies downstream purification (Zhang *et al.*, 2019). Additionally, KOH is versatile across various feedstocks, including animal fats and vegetable oils. It is also more effective than NaOH, as potassium soaps formed during transesterification are softer, leading to less clogging during separation.

The next section will focus on the Box-Behnken design, a response surface methodology (RSM)-based experimental design, used to optimise key parameters in biodiesel production. Experiments are conducted by varying methanol volume, catalyst concentration and reaction time. RSM aims to optimise these process parameters, solving regression model equations using Design Expert (version 13) software and analysing three-dimensional surface plots to maximise biodiesel yield. Analysis of variance (ANOVA) helps identify the dominant factors influencing biodiesel production efficiency.

Design of Experiments (DOE)

Simsek *et al.* (2022) used the DOE as a systematic approach to test and analyse the effects of various factors on the outcome of a product or process. DOE assists in identifying significant factors and their optimal levels by systematically adjusting factor levels. This method enables the examination of specific results under various experimental conditions, facilitating the improvement of the process (Gupta *et al.*, 2022). ANOVA is commonly employed in experimental designs to visually evaluate the effects of different factors and their interactions on the response variables (Parak *et al.*, 2022).

Response Surface Methodology (RSM)

RSM is a statistical technique used to model and optimise the relationship between independent variables and a response. In biodiesel synthesis from palm stearin, RSM helps optimise key parameters

such as reaction time, catalyst concentration and methanol concentration to maximise yield. Experimental designs like the Box-Behnken Design (BBD) vary these variables systematically. A polynomial model is then used to represent the relationship, with regression analysis identifying the optimal conditions. The goal is to reduce the number of experiments while effectively exploring factor ranges.

Once optimal conditions are determined, confirmatory experiments validate the results to ensure reliability for real-world applications (Buasri *et al.*, 2024; Loryuenyong *et al.*, 2024; Yusoff *et al.*, 2022). Overall, RSM provides a systematic method for enhancing biodiesel production by building predictive models and improving yield and quality (Karimi & Saidi, 2022; Ngige *et al.*, 2023).

Box-Behnken Design (BBD)

BBD is a widely applied response surface design (RSD) in statistics, commonly used in the DOE to represent the relationships between multiple input factors and one or more output variables. The BBD offers advantages over full factorial designs because it requires fewer experiments while still providing reliable estimates of variable interactions (Manimaran *et al.*, 2022). This design proves particularly useful for determining the optimal conditions in product development and process optimisation.

BBD functions by selecting a set of independent variables, or factors, and assigning three levels to each-usually at the midpoint of the desired range (Kober *et al.*, 2022). These levels are then combined to create a subset of possible experiments, each exploring different combinations of factors. The value of this approach lies in its ability to optimise a response variable by analysing the interactions between input factors and output responses (Joorasty *et al.*, 2022).

The authors chose BBD over Central Composite Design (CCD) for several reasons: BBD requires fewer experimental runs, making it more efficient, especially when resources are limited. Additionally, BBD lacks axial points, which simplifies the interpretation of interactions among variables. It is well-suited for fitting second-order (quadratic) models, effectively capturing the relationships among methanol volume, catalyst quantity and reaction time without risking overfitting. BBD also provides a balanced design, ensuring equal examination of factors and allowing for flexibility in factor levels, enhancing the ability to identify optimal conditions for biodiesel production. Overall, BBD offers a robust and straightforward framework for this study's objectives.

In summary, applying BBD to optimise biodiesel synthesis from palm stearin is a pragmatic and effective strategy, especially considering the complexity of the process and resource constraints. Study by Buasri *et al.* (2023) demonstrates the efficacy of BBD in similar scenarios, highlighting its utility in achieving optimal experimental designs.

The novelty of this study lies in the comprehensive optimisation of palm stearin transesterification processes using RSM and BBD. While extensive research exists on biodiesel synthesis from palm oil and other raw materials, the potential of palm stearin-a by-product of palm oil fractionation-remains underexplored. This study identifies the most favourable conditions for biodiesel production while also enhancing the sustainable use of palm stearin, thereby increasing the value of a typically low-value by-product.

In addition, the application of RSM and BBD in this study provides a systematic and efficient approach for evaluating the combined effects of key process variables-namely methanol concentration, catalyst (KOH) loading and reaction time-on biodiesel production. This methodology allows for the identification of optimal conditions that maximise biodiesel yield while minimising the consumption of reactants and energy.

This study aimed to improve the transesterification process for biodiesel production from palm stearin through a systematic experimental methodology. A BBD was employed within the framework of RSM to model the interactions among critical process variables (methanol volume, catalyst quantity and reaction time) and their effects on biodiesel yield. We developed a quadratic model to predict optimal conditions for maximum biodiesel output. The research also involved an analysis of the physicochemical properties of the produced biodiesel to evaluate its suitability for practical applications. Overall, this study sought to enhance the understanding of biodiesel optimisation and to establish a more efficient production process using palm stearin as a feedstock.

MATERIALS AND METHODS

Materials

Fractionation is a process that yields palm stearin, a solid fraction of palm oil. Fractionation involves heating and cooling palm oil to separate its various components according to their melting points. Palm stearin has a higher melting point than other fractions of palm oil, such as palm olein and is therefore solid at room temperature.

The palm stearin used in this study was procured from Murugan Oil Mill, Namakkal, India. The chemicals used in the process were methanol

with a purity of 99.85% and grade AA, and KOH pellets with a purity of 85.00%. The chemicals, methanol and KOH, were obtained from Blulux Laboratories in Faridabad, India and Chemind Laboratory Chemicals in Thrissur, India respectively.

Palm stearin was stored in airtight containers at a temperature below its melting point of 52°C to maintain its solid state. The containers of palm stearin were placed in a dry environment to prevent moisture absorption and air exposure. Moisture can lead to hydrolysis, forming FFA that negatively affect the transesterification process (Bustamam *et al.*, 2022). To avoid contamination, handling and transferring of palm stearin was done using a clean, stainless-steel ladle.

Palm stearin was stored in airtight containers at a temperature below its melting point of 52°C to maintain its solid state. The containers of palm stearin were placed in a dry environment to prevent moisture absorption and air exposure. Moisture can lead to hydrolysis, forming FFA that negatively affect the transesterification process (Bustamam *et al.*, 2022). To avoid contamination, transferring and handling palm stearin was done by using a clean, stainless-steel ladle.

Biodiesel Production by Transesterification Method

The equipment used for the transesterification reaction consisted of a 1,000 mL Erlenmeyer flask, a thermometer and a magnetic stirrer. The palm stearin was originally in a solid state. Every sample preparation began with melting palm stearin at 50°C and pouring 1,000 mL of the melted palm stearin into an Erlenmeyer flask. We blended the melted palm stearin with the homogenous potassium methoxide solution, which was prepared by reacting the catalyst KOH and methanol, and the reaction mixture in the flask was subsequently stirred using a magnetic stirrer. The temperature of

the reaction mixture was maintained below 60°C (the boiling point of methanol).

After the specified reaction time (45, 60, or 90 min), the reaction products (methyl ester and glycerol) were transferred to a separating funnel and allowed to settle for 24 hr. Then, high-density glycerol settled at the bottom of the funnel and was removed using a valve in the separator funnel. The methyl ester phase was washed with water to eliminate any unwanted impurities. Then the methyl ester was heated to 105°C to remove any moisture and to obtain pure biodiesel. The schematic diagram of the transesterification process is shown in *Figure 1*. The physicochemical properties of the produced biodiesel were determined using the standard methods mentioned in *Table 1*.

The characterisation of biodiesel was conducted using gas chromatography-mass spectrometry (GC-MS) to identify the fatty acid methyl esters (FAME) content. The Agilent 8890 GC System (Agilent Technologies, Santa Clara, CA, USA), equipped with a quadrupole mass selective (Agilent 5977B MSD) detector, was employed for capillary GC/MS analysis. A DB-5MS capillary column (30.00 m, 0.25 mm ID, 0.25 µm film thickness) was used for the separation. The injector was operated in split mode with a split ratio of 7500:1 and the injection volume was set at 1 µL.

The column temperature sequence involves holding the initial temperature at 60°C for 2 min, then increasing it by 10°C/min to 200°C and holding it for 5 min. Lastly, the temperature is increased by 5°C/min to 280°C and held for 10 min. Helium, with a constant flow rate of 1 mL/min, served as the carrier gas. In mass spectroscopy, the electron impact mode operates at 70 eV. The quadrupole temperature at 150°C, the ion source temperature at 230°C, and the transfer line temperature at 280°C are maintained. Mass range in full scan mode from m/z 50-550 to prevent solvent interference, with a solvent delay of 3 min is done.

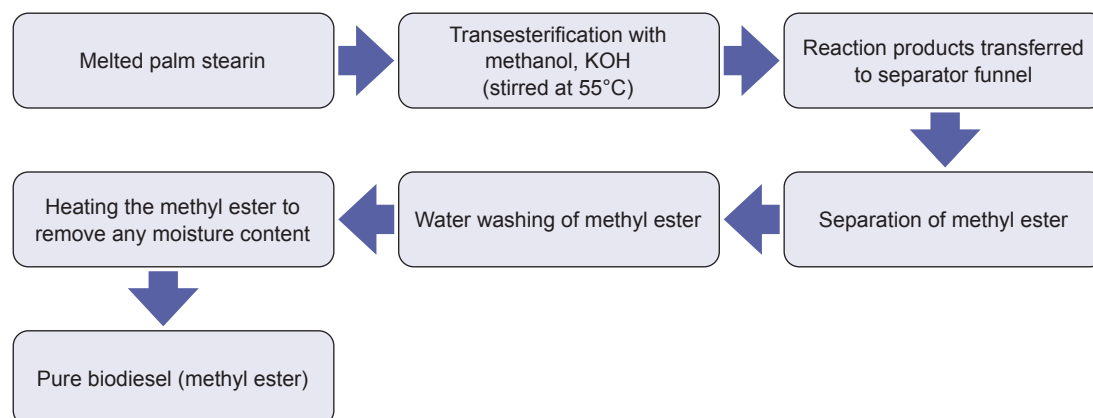


Figure 1. Schematic diagram of the transesterification process.

A calibration curve is generated by preparing a set of fatty acid methyl ester (FAME) standards in hexane at five different concentrations. The concentrations are 0.1, 0.2, 0.5, 1.0 and 2.0 mg/mL. To make the standard solutions, a concentrated FAME solution is diluted with hexane and then put through a 0.45 μm PTFE syringe filter before it is analysed. 1 μL of each standard solution was injected into the GC/MS system, and the peak areas corresponding to each concentration were recorded. Agilent MassHunter software conducts the data acquisition and processing. The compounds are identified by comparing retention times and mass spectra with standards and the NIST library.

Experimental Conditions by BBD for Biodiesel Yield

The three-level, two-factor BBD was identified as appropriate for designing the experimental settings in this research. Methanol (A) volume was varied at three levels: 200 (-1), 225 (0) and 250 mL (+1). The catalyst (B) was set at 8 (-1), 10 (0) and 12 g (+1). Similarly, reaction time (C) was tested

at three durations: 45 (-1), 60 (0) and 90 min (+1). The experimental conditions proposed by RSM for biodiesel yield, in coded values, are presented in *Table 2*.

Statistical Summary of Model

In the present study, a quadratic model was selected to fit the experimental data based on statistical indicators, such as R^2 and adjusted R^2 (Adj- R^2). Although a cubic model demonstrated higher R^2 and Adj- R^2 values, aliasing problems hindered the distinction between the individual effects of the variables, thereby making the cubic model unsuitable. The linear relationship yielded R^2 and Adj- R^2 values of 0.2126 and 0.0960, respectively, clearly indicating its inadequacy for modelling the experimental data. Therefore, the quadratic model was determined to be the most appropriate, providing a better fit with an R^2 of 0.9967 and an Adj- R^2 of 0.9812 at a 99% confidence level. *Table 3* shows that the quadratic model fits the data significantly better than the linear or cubic models, which supports its choice for further analysis.

TABLE 1. DESCRIPTION OF STANDARD METHODS OF TESTING PARAMETERS

No.	Test parameters	Methods	Description
1.	Ash content	ASTM D482-13	The ash content was determined by weighing the residue remaining after the combustion of the biodiesel sample at 775°C.
2.	Density @ 15°C	IS:1448 Part 32: 2019	The density of the biodiesel was measured using a hydrometer at 15°C.
3.	Moisture content	IS:1448 Part 40: 2015	The moisture content was determined using the Karl Fischer titration method.
4.	Kinematic viscosity @ 40°C	ASTM D 445: 2015	The kinematic viscosity of the biodiesel was measured at 40°C using a capillary viscometer.
5.	Cetane index	ASTM D976-06	The cetane index was calculated based on the density and distillation range of the biodiesel.
6.	Acidity	IS:1448 Part 2: 2007	The acidity of the biodiesel was measured by titration with KOH.
7.	Sulphur content	IS:1448 Part 33: 1991	The sulphur content was determined using an X-ray fluorescence spectrometer.
8.	Flash point	IS 1448 Part 20: 1998	The flash point of the biodiesel was determined using a Pensky-Martens closed cup tester.
9.	Fire point	IS 1448 Part 20: 1998	The fire point was measured as the temperature at which the biodiesel produced a flame when ignited.
10.	Sulphated ash	ASTM D874-13	The sulphated ash content was measured by combustion of the sample and subsequent treatment with sulfuric acid.
11.	Relative density @ 15°C	IS:1448 Part 32: 2019	The relative density of the biodiesel was determined using a hydrometer at 15°C.
12.	Net calorific value	IS:1448 Part 6: 1984	The net calorific value was measured using a bomb calorimeter.

TABLE 2. BBD PROPOSED EXPERIMENTAL SETTINGS FOR BIODIESEL YIELD

Variable	Real values			
	Code	-1	0	1
Methanol (mL)	A	200	225	250
Catalyst (g)	B	8	10	12
Reaction time (min)	C	45	60	90

RESULTS AND DISCUSSION

Fit Statistics

Table 4 presents the fit statistics derived from Design Expert version 13. The close agreement between the Adj-R² (0.9967) and predicted R² (0.9812) confirms the robustness of the quadratic model. The adequate precision value of 57.8018, well above the threshold of 4, demonstrates a strong signal-to-noise ratio, which is crucial for model accuracy in navigating the design space. Table 5 presents the experimental conditions proposed by the BBD for optimising biodiesel yield. It includes both coded and actual values for methanol, catalyst and reaction time, as well as the actual and predicted yields. The strong correlation between the actual and predicted biodiesel yields further validates the model's reliability.

Based on the model evaluation, the quadratic model [Equation (1)], expressed in coded terms, is presented below:

$$\begin{aligned} \text{Biodiesel yield} = & 910.00 + 99.56(A) + & (1) \\ & 75.63(B) + 82.66(C) + \\ & 75.60(A*B) + 65.00(A*C) \\ & + 51.75 (B*C) - 20.01(A)^2 \\ & - 13.97(B)^2 - 24.39(C)^2 \end{aligned}$$

Equation (1) illustrates the relationship between biodiesel yield and the three key process factors: Methanol (A), catalyst (B) and reaction time (C). The positive coefficients of the linear and interaction terms indicate that increasing the factors, within the tested range, contributes positively to biodiesel yield.

TABLE 3. STATISTICAL SUMMARY

Source	Sequential <i>p</i> -value	Adj-R ²	Predicted R ²	
Linear	0.1384	0.2126	0.0960	
Quadratic	< 0.0001	0.9967	0.9812	Suggested
Cubic		1.0000		Aliased

TABLE 4. FIT STATISTICS WERE OUTPUT BY DESIGN EXPERT VERSION 13

Standard deviation	4.87	R ²	0.9988
Mean	790.67	Adj-R ²	0.9967
Coefficient of variation (%)	0.6164	Predicted R ²	0.9812
		Adequate precision	57.8018

TABLE 5. EXPERIMENTAL CONDITIONS PROPOSED BY BBD

Run	Coded values of variables			Actual level of variable			Actual	Predicted
	Methanol (mL)	Catalysts (g)	Reaction time (min)	Methanol (mL)	Catalysts (g)	Reaction time (min)		
1	-1	0	1	200	10	90	690	691.25
2	0	-1	1	225	8	90	745	748.13
3	-1	1	0	200	12	60	705	708.13
4	1	1	0	250	12	60	890	894.38
5	-1	0	-1	200	10	45	680	680.00
6	1	0	1	250	10	90	850	850.00
7	0	0	0	225	10	60	910	913.40
8	1	0	-1	250	10	45	760	758.75
9	0	0	0	225	10	60	910	913.40
10	1	-1	0	250	8	60	780	776.88
11	0	-1	-1	225	8	45	720	724.38
12	-1	-1	0	200	8	60	730	725.63
13	0	0	0	225	10	60	910	913.40
14	0	1	-1	225	12	45	750	746.88
15	0	1	1	225	12	90	830	825.63

The equation, expressed in the terminology of coded factors, can be applied to predict responses at different levels of each factor. By default, a high level of the factors is coded as +1, while a low level is coded as -1. By correlating the factor coefficients, the coded equation can be used to calculate the relative significance of the factors. In terms of actual factors, this same equation is capable of estimating responses at different levels of each factor. The levels for each factor must be indicated in their original units. Therefore, the coefficients are adjusted to fit the units of each factor, and the correlation coefficient is assessed at the design centre point. Thus, an equation should be used to calculate the comparative impact of each variable.

Model Accuracy Check

Table 6 displays the ANOVA results for the obtained model. ANOVA is an analytical technique that uses a t-test and an F-test to conclude the significance of a model and its variables. Using a *p*-value threshold, the Student's t-test was applied to evaluate the significance of the correlation coefficients. Larger F-values and smaller *p*-values generally demonstrate significant coefficient conditions. The F-value, standing at 471.23 with a *p*-value below 0.0001, indicates that only a minuscule fraction of the variability could justify such a significant F-value. Significant model terms have *p*-values below 0.0500. In this case, significant model terms include A, B, C, AB, AC, BC, A², B² and C². Model terms are not significant if the *p*-value is greater than 0.1000. Model reduction may be helpful if the model has many superfluous terms (excluding those required to maintain hierarchy).

The RSM design predicts a biodiesel yield value of 913.40 mL, which corresponds to a yield percentage of 89.59%, under conditions of 225 mL of methanol, a catalyst concentration of 10 g and a reaction time of 60 min. According to Figure 2, the

desirability value is 1 under these conditions, with a biodiesel yield of 910 mL, equating to a yield percentage of 89.25%. In contrast, Hussanai and Kittisak (2023) predicted the highest yield of 96.73% and achieved a yield percentage of 92.74% in their experiment on the transesterification of palm oil with KOH catalyst supported on palm kernel shell ash. The RSM predicted value of biodiesel yield is found to be 99% accurate compared to the experimental result.

To establish an adequate model, an accuracy check is necessary. The comparison of anticipated and experimental biodiesel yields serves as evidence for the model's accuracy. The linear relationship between experimental and predicted biodiesel yield is shown in Figure 3a. A normal residual plot was also obtained between internally studentised residuals and normal probability (%). The internal residuals can be used to calculate the standard deviations between the predicted and experimental values. The residuals are then analysed to determine if the model aligns with the ANOVA interpretation. The relationship between the internally studentised residuals and normal probability (%) is depicted in Figure 3b. The straight line indicates that no reaction conversion is needed and that normality is not affected.

Response Analysis

Figure 4 depicts the interactions between biodiesel yield and these three factors. Each graph represents the impact of two parameters over their respective investigated intervals, with the third parameter set to zero. The response surface illustrates each factor's tendency to affect biodiesel yield. The contour plot's shape reveals the type and extent of factor interactions. An elliptical contour plot suggests a significant interaction, while a circular contour plot signifies a minor effect (Khan *et al.*, 2022).

TABLE 6. ANOVA CONSEQUENCES FOR THE OBTAINED MODEL

Source	Sum of squares	Degree of freedom	Mean square	F-value	<i>p</i> -value	Characteristic
Model	1.007E+05	9	11,191.62	471.23	< 0.0001	Significant
A-A	28,203.12	1	28,203.12	1,187.50	< 0.0001	
B-B	5,000.00	1	5,000.00	210.53	< 0.0001	
C-C	5,253.13	1	5,253.13	221.18	< 0.0001	
AB	4,556.25	1	4,556.25	191.84	< 0.0001	
AC	1,600.00	1	1,600.00	67.37	0.0004	
BC	756.25	1	756.25	31.84	0.0024	
A ²	20,769.23	1	2,0769.23	874.49	< 0.0001	
B ²	12,744.23	1	12,744.23	536.60	< 0.0001	
C ²	29,907.69	1	29,907.69	1,259.27	< 0.0001	
Residual	118.75	5	23.75			
Lack of fit	300.00	3	100.00	1.43	0.30	Not significant

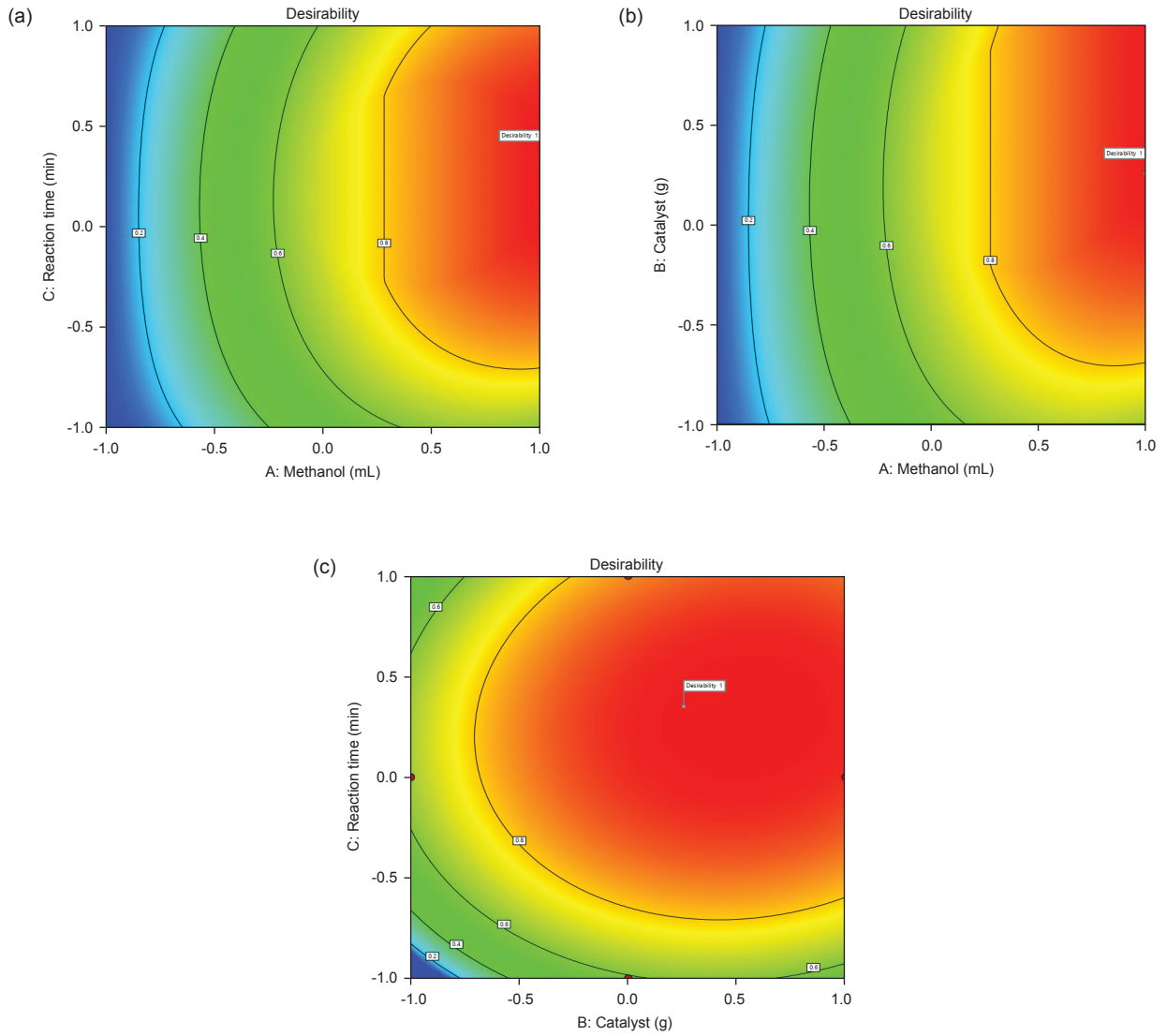


Figure 2. (a) Optimisation plot for methanol and reaction time, (b) methanol and catalyst and (c) reaction time and catalyst for the yield of biodiesel.

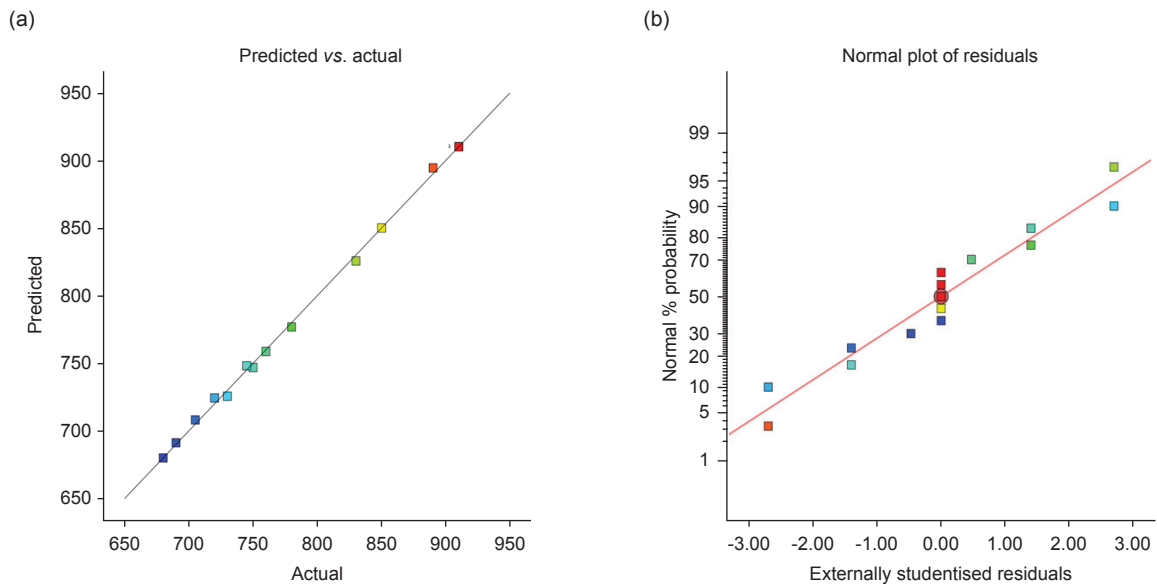


Figure 3. (a) Biodiesel yield predictions versus experimental results and (b) relationship between normal probability (%) and externally studentised residuals is depicted by a normal plot of residuals.

The plots show that biodiesel yield increases as methanol concentration increases. An increase in methanol above the 225 mL level, on the other hand, does not result in an additional increment in biodiesel yield but instead leads to a slight reduction. Therefore, there is an optimal methanol concentration of 225 mL and a catalyst concentration of 10 g. Concerning the effect of catalyst concentration, the biodiesel yield rises

with increasing catalyst concentration from 8-12 g. Conversely, beyond this concentration, the biodiesel yield begins to decrease. Thus, there is an optimal catalyst concentration of 10 g and a reaction time of 60 min. Regarding the effect of reaction time, raising the reaction time from 45-60 min tends to increase the biodiesel yield. Moreover, once this concentration is reached, the biodiesel yield begins to decline (Bai *et al.*, 2022).

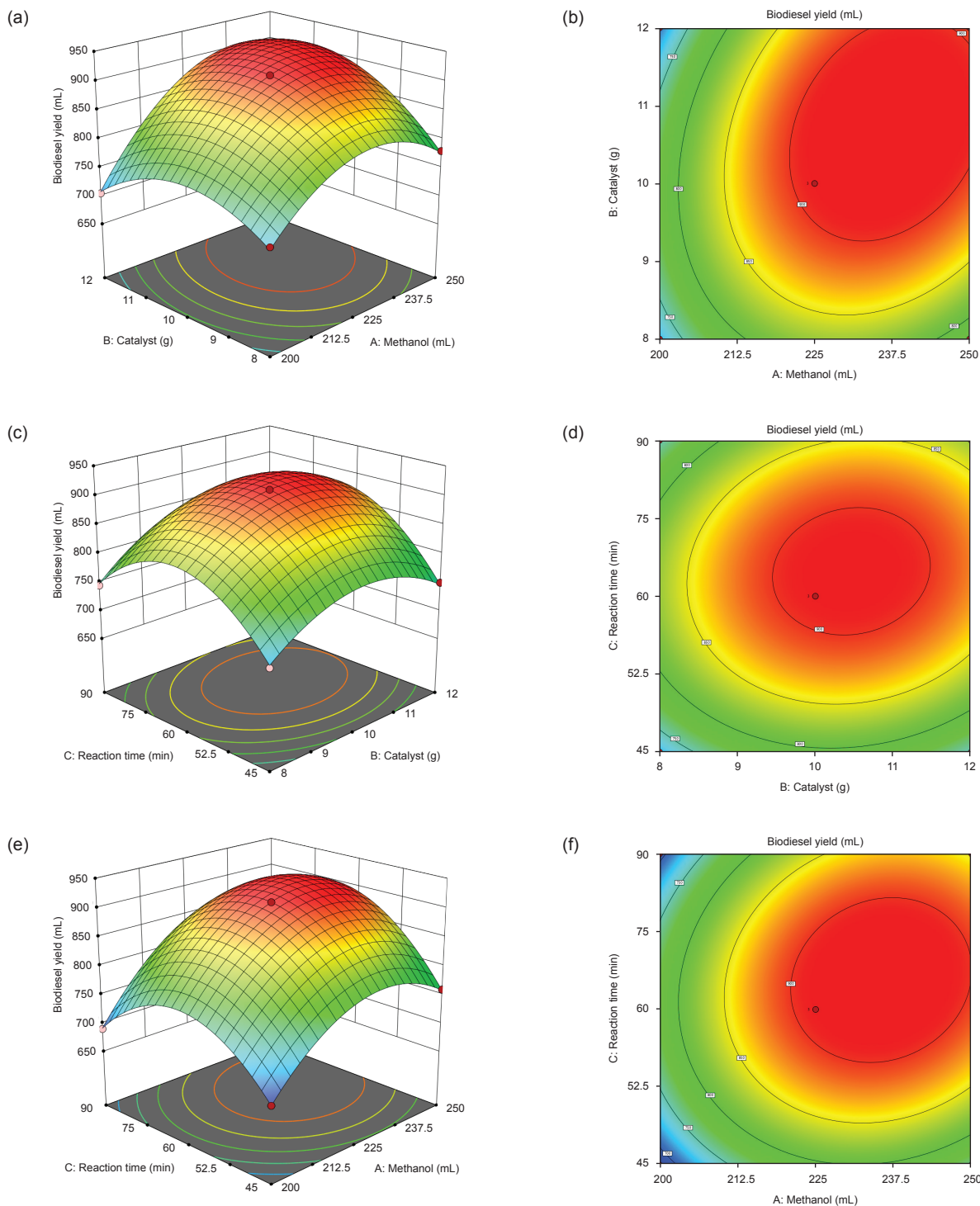


Figure 4. (a) Methanol and catalyst combined for biodiesel yield response surface, (b) methanol and catalyst contour plot of the expected biodiesel yield, (c) catalyst and reaction time combined for biodiesel yield response surface, (d) catalyst and reaction time contour plot of the expected biodiesel yield, (e) methanol and reaction time combined for biodiesel yield response surface and (f) reaction time combined contour plot of the expected biodiesel yield.

Therefore, there is an optimal reaction time of 60 min and a methanol concentration of 225 mL. At 225 mL methanol, with a 10 g catalyst and a reaction time of 60 min, the maximum biodiesel yield of 910 mL is achieved.

BBD necessitates fewer experimental runs and can effectively simulate quadratic relationships; nevertheless, it may underperform in situations with high values or pronounced non-linearities, where CCD may better capture intricate features. Future research could investigate hybrid methodologies that integrate the advantages of both CCD and BBD or utilise sophisticated techniques such as machine learning models for optimisation to uncover additional improvements in biodiesel production efficiency.

Biodiesel Yield

Effect of catalyst concentration. A stirrer blends the catalyst and methanol in a small reactor. The oil should first be charged into the reactor, after which the KOH/methanol mixture is added to the oil. Triglycerides may take longer to completely convert to biodiesel and glycerol if there is insufficient catalyst concentration, which can cause slower reaction rates. This prolonged reaction time may raise processing expenses and decrease manufacturing efficiency. Lower catalyst concentrations may cause the conversion of triglycerides to biodiesel to be incomplete, thereby reducing biodiesel production. The unreacted triglycerides that are still present in the reaction mixture necessitate more processing stages or reagents to achieve the required degree of conversion, which might escalate the cost and complexity even further. A higher catalyst concentration may cause the usage of more reactants than necessary, hence might lower the output of biodiesel. This occurs because of the excess catalyst, which can potentially trigger unintended reactions like saponification, reducing the output of biodiesel by forming soap. Since catalysts frequently account for a sizeable percentage of the total costs associated with producing biodiesel, using more catalysts than necessary raises production costs. Oil, alcohol and water combinations that are stable can create emulsions when there is an overabundance of catalysts present. Emulsions may obstruct the biodiesel's ability to separate from the reaction mixture, complicating subsequent steps and adding time and energy to the purifying process. Theam *et al.* (2015) achieved the highest yield at 1.00% (w/w) catalyst loading for the transesterification of palm stearin with a metal-doped methoxide solid catalyst. Verma and Sharma (2016) achieved the highest yield at 1.22% (w/w) catalyst loading for the transesterification

of karanja oil with methanol and KOH as catalysts. The optimum concentration of the catalyst, KOH, for the highest biodiesel yield in this study is 10 g, corresponding to a catalyst loading of 1.12% (w/w), which falls within the range specified by Verma and Sharma (2016).

Effects of methanol. The amounts of methanol (200, 225 and 250 mL) were utilised in this experiment. The molar ratio is the most significant variable that affects conversion efficiency and biodiesel production costs. The conversion efficiency is defined as the process yield expressed as a percentage. An optimum molar ratio minimises excess methanol, which can cause side reactions and lower the yield while ensuring that there is enough methanol to react with all the fatty acid esters found in the palm stearin. The side reactions, including the production of soap and fatty acid methyl esters with shorter carbon chains, might result from using too much methanol. These side reactions have the potential to impair the biodiesel product's quality and make the separation procedure more difficult (Verma & Sharma, 2016). For the highest yield of 910 mL, the transesterification process uses a molar ratio of 5.58:1 between methanol and palm stearin. Theam *et al.* (2015) achieved the highest yield at a molar ratio of 6:1 between methanol and palm stearin for the transesterification of palm stearin with a metal-doped methoxide solid catalyst. Vyas *et al.* (2011) optimised the molar ratio to 6:1 for the transesterification of jatropha oil with methanol. The presence of both water and FFA tends to promote saponification (Danane *et al.*, 2022). Therefore, the oils and alcohols must mostly be anhydrous.

Effect reaction time. We investigated the impact of reaction time on palm stearin transesterification efficiency in biodiesel production. When transforming palm stearin, working with a reaction time that is below ideal can lead to a variety of problems, including inadequate phase separation, increased contaminants, inconsistent product quality and incomplete conversion. Shorter reaction periods may lead to the formation of soap, mono- and diglycerides and FFA. These contaminants may have a negative impact on the quality and characteristics of the biodiesel product, resulting in reduced fuel efficiency and potential engine issues. When transforming palm stearin, running at a reaction time longer than ideal can lead to resource waste, lower reaction selectivity, higher energy consumption, product deterioration and ineffective separation. Prolonging the reaction beyond the required duration results in excessive utilisation of catalysts, energy and raw materials, leading to decreased productivity and increased expenses in

the production process. Prolonged reaction times can lead to the formation of unwanted by-products, such as soap and glycerides, due to side reactions. This lowers the transesterification process's selectivity, resulting in lower biodiesel purity and yield. Therefore, to maximise the efficiency of biodiesel production while minimising expenses, it is imperative to carefully manage and optimise the reaction time. The optimum reaction time for the highest biodiesel yield is 60 min. Theam *et al.* (2015) achieved the highest yield at 180 min for the transesterification of palm stearin with a metal-doped methoxide solid catalyst. Vyas *et al.* (2011) achieved the highest yield at 30 min for the transesterification of jatropha oil with methanol, and Verma and Sharma (2016) achieved it at 90 min for the transesterification of karanja oil with methanol.

The molar ratio of methanol to palm stearin, as well as the weight-to-weight (w/w) catalyst loading, demonstrate consistency with Theam *et al.* (2015), Verma and Sharma (2016) and Vyas *et al.* (2011), affirming adherence to established practices in the transesterification process. The validation analysis of the quadratic response was carried out by performing an experimental study to verify the predicted optimised parameters obtained from Equation (2):

$$\begin{aligned} \text{Biodiesel yield} = & 910.00 + 99.56(225) + & (2) \\ & 75.63(10) + 82.66(60) \\ & + 75.60(225 \cdot 10) + \\ & 65.00(225 \cdot 60) + 51.75(10 \cdot 60) \\ & - 20.01(225)^2 - 13.97(10)^2 - \\ & 2 \cdot 4.39(60)^2 = 913.40 \text{ mL} \end{aligned}$$

Attaining an 89.25% biodiesel yield from palm stearin offers significant benefits in the industrial synthesis of biodiesel. From an economic perspective, elevated yield rates mean that a greater proportion of the raw feedstock is transformed into usable fuel, resulting in substantial cost savings on raw materials. This directly reduces the need for acquiring supplementary feedstock and lowers the overall per-unit manufacturing cost of biodiesel. In an industrial setting, efficient feedstock utilisation increases throughput, reducing the necessity for prolonged processing times or multiple reaction phases. This leads to decreased energy consumption and less wear on equipment, therefore lowering maintenance expenses and improving the long-term sustainability of industrial operations. Moreover, reduced energy usage correlates with a diminished carbon footprint, thereby enhancing the environmental benefits of biodiesel as a cleaner fuel alternative.

In addition to cost reductions, such a high yield ensures efficiency improvements across various industrial applications. An optimised transesterification process requires fewer resources to produce the same volume of biodiesel, potentially motivating more industries to adopt biodiesel as a viable alternative to conventional fossil fuels. Furthermore, a more efficient production process makes the scaling up of biodiesel production more feasible, enabling increased industrial output without a corresponding rise in operational costs or environmental impact. This is particularly crucial for industries aiming to achieve sustainability goals while maintaining profitability. Consequently, achieving high biodiesel yields not only improves economic feasibility but also strengthens biodiesel's position as a competitive, green energy source in both local and global energy markets.

Biodiesel Characteristics and Properties

Biodiesel properties. We conducted laboratory tests to determine the physical properties of the biodiesel. Table 7 provides the standards used for the various properties of diesel and palm stearin biodiesel, along with ASTM D6751 (for the United States) and EN14214 (for the European Union) standards (DieselNet, 2009).

Palm stearin biodiesel meets the criteria for ash content, density @ 15°C, moisture content, kinetic viscosity @ 40°C, acidity, flash point, fire point, sulphated ash and relative density @ 15°C. The cetane number of palm stearin biodiesel is slightly below both ASTM D6751 and EN14214 standard values. The sulphur content of palm stearin biodiesel exceeds both ASTM D6751 and EN14214 standard values. The net calorific value of palm stearin biodiesel is slightly below the EN14214 standard value.

Blending diesel with palm stearin biodiesel at a ratio of 80% diesel to 20% biodiesel can meet ASTM D6751 and EN14214 minimum criteria. Diesel usually has a low sulphur level or complies with Ultra-Low Sulfur Diesel (ULSD) regulations. The total sulphur level of the mix drops by blending with diesel, which has a lower sulphur concentration, assisting in meeting the allowable limitations. In general, diesel fuel has a greater cetane number than biodiesel. Adding diesel to the mix may raise its cetane index and improve the blend's ignition and combustion properties. Diesel's high cetane number will still have a major effect on the blend, even though biodiesel alone helps to improve cetane (Sakkampang *et al.*, 2023).

In comparison to biodiesel, diesel fuel has greater flash and fire points. Combining the blend with diesel will increase its fire and flash points, thereby enhancing handling and storage

safety. By modifying the blend ratios to satisfy the required criteria, blending with diesel can also assist in producing the right density, viscosity and other qualities. Blending biodiesel with diesel can counteract its increased viscosity and bring it within the permissible limit (Sakthivel *et al.*, 2018).

Biodiesel characteristics. The GC-MS test can provide information about the FAMES present in the biodiesel sample and also identify any impurities like glycerol or water (Manojkumar *et al.*, 2022). If the biodiesel passes the quality criteria established by regulatory agencies like the American Society for Testing and Materials (ASTM), the findings of the GC-MS test can be used to make that determination. The GC-MS analysis that was performed is shown in *Figure 5*. *Table 8* includes the sixteen chemicals found during the analysis. Five of the sixteen components are major, while the other twelve are minor.

Using the MS database library as a base, these peaks can be identified. Several derivatives of hexadecanoic acid, including methyl ester (C₁₇H₃₄O₂), were found in the highest concentration (24.79%). The MS database allows for the identification of these peaks, which include 9-Octadecenoic acid (Z)-, methyl ester (C₁₉H₃₆O₂) (21.90%), 9,12-Octadecadienoic acid (Z, Z)-, methyl ester (C₁₉H₃₄O₂) (13.64%), methyl stearate (C₁₉H₃₈O₂) (13.20%) and methyl tetradecanoate (C₁₅H₃₀O₂) (11.16%).

The FAME content in palm stearin biodiesel is shown in *Table 9*. In the biodiesel made from palm stearin, the saturated FAME percentage is 59.19%, the unsaturated FAME level is 38.47% and the overall FAME content is 97.66%. The remaining 2.34% of the palm stearin biodiesel comprises other substances or contaminants, such as methanol,

water, glycerides, glycerol and small amounts of other components. These substances may be by-products, contaminants, or unreacted starting components.

Higher levels of saturated FAME in biodiesel are commonly associated with higher viscosities, improved oxidative stability, higher pour points and higher cloud points. Saturated FAME typically has higher melting temperatures and viscosities than unsaturated FAME. This can result in poorer low-temperature properties and increased viscosity, which can affect engine performance and flow characteristics, particularly in cold weather. Over time, biodiesel with saturated FAME exhibits superior oxidative stability because it is generally more resistant to oxidation than unsaturated FAME. A higher saturated FAME level in biodiesel raises its cloud point and pour point, which may impact its cold flow characteristics and suitability for use in colder regions.

Higher levels of unsaturated FAME in biodiesel are commonly associated with lower viscosities, poorer oxidative stability, lower pour and cloud points, and higher cetane numbers. When compared to saturated FAME, unsaturated FAME often has greater cetane values, which enhance biodiesel's ignition quality and combustion properties, leading to smoother engine operation and lower emissions.

In general, an elevated overall FAME concentration results in biodiesel having a higher energy content per unit volume, which provides more energy for combustion and may boost fuel efficiency. FAME components contribute to the lubricity of biodiesel, reducing engine wear and tear and prolonging engine life. Higher FAME content in biodiesel tends to make it more biodegradable, which lessens the impact of spills or leaks on

TABLE 7. BIODIESEL PROPERTIES

No.	Test parameters	Unit	Petroleum diesel	ASTM D6751	EN14214	Palm stearin biodiesel	Test method
1	Ash	% by mass	0.01	≤0.02%	≤0.02%	0.02	ASTM D 482:2013
2	Density @ 15°C	g/cm ³	0.85	0.82-0.90	0.86-0.90	0.8670	IS:1448 part 32:2019
3	Moisture	% by mass	0.01	≤0.05%	≤0.02%	BLQ	IS:1448 part 40:2015
4	Kinematic viscosity @ 40°C	mm ² /s (cSt)	4.5	1.9-6.0	3.5-5.0	4.7	ASTM D 445:2015
5	Cetane index	-	55	≥47	≥51	42.2	ASTM D976-06
6	Acidity	mg of KOH/g	0.02	≤0.50	≤0.50	0.2	IS:1448 part 2:2007
7	Sulphur	% by mass	0.001	≤0.0015	≤0.001	0.08	IS:1448 part 33:1991
8	Flash point	°C	96	≥93	≥95	170	IS 1448 Part 20:1998
9	Fire point	°C	96	N/A	≥140	179	IS 1448 Part 20:1998
10	Sulphated ash	% by mass	0.01	≤0.02	≤0.02	0.02	ASTM D 482:2013
11	Relative density @ 15°C	-	0.85	N/A	0.860-0.900	0.8678	IS:1448 part 32:2019
12	Net calorific value	cal/g	10038.241	N/A	≥ 8556.40	8503	IS:1448 part 6:1984

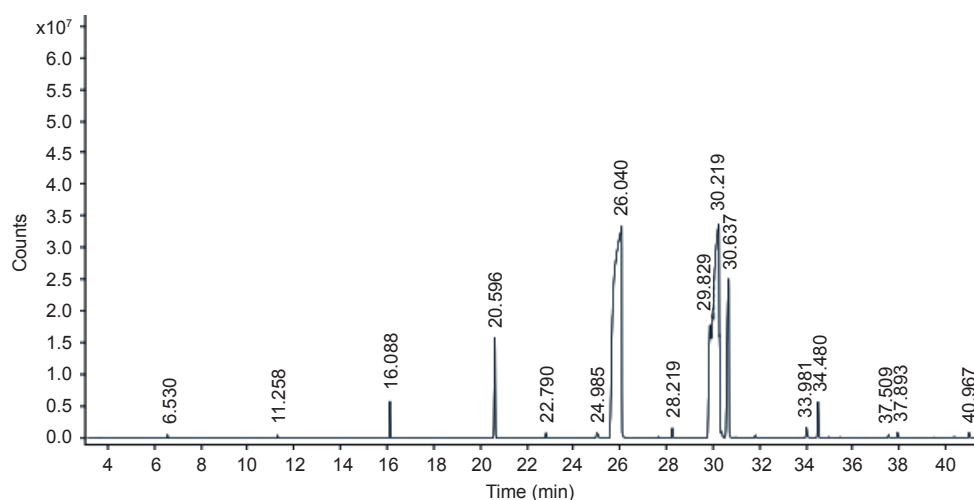


Figure 5. GC-MS test outcomes for biodiesel.

TABLE 8. ELEMENTS ACQUIRED IN GCMS RESULT

No.	Compound name	Peak	Area in %	Chemical formula
1	Octanoic acid, methyl ester	6.530	0.29	C ₉ H ₁₈ O ₂
2	Decanoic acid, methyl ester	11.258	0.29	C ₁₁ H ₂₂ O ₂
3	Dodecanoic acid, methyl ester	16.088	3.60	C ₁₃ H ₂₆ O ₂
4	Methyl tetradecanoate	20.596	11.16	C ₁₅ H ₃₀ O ₂
5	Pentadecanoic acid, methyl ester	22.790	0.63	C ₁₆ H ₃₂ O ₂
6	Methyl hexadec-9-enoate	24.985	1.19	C ₁₇ H ₃₂ O ₂
7	Hexadecanoic acid, methyl ester	26.040	24.79	C ₁₇ H ₃₄ O ₂
8	Heptadecanoic acid, methyl ester	28.219	1.34	C ₁₈ H ₃₆ O ₂
9	9,12-Octadecadienoic acid (Z, Z)-, methyl ester	29.829	13.64	C ₁₉ H ₃₄ O ₂
10	9-Octadecenoic acid (Z)-, methyl ester	30.219	21.90	C ₁₉ H ₃₆ O ₂
11	Methyl stearate	30.637	13.20	C ₁₉ H ₃₈ O ₂
12	cis-Methyl 11-eicosenoate	33.981	1.74	C ₂₀ H ₃₈ O ₂
13	Eicosanoic acid, methyl ester	34.480	4.39	C ₂₁ H ₄₀ O ₂
14	Glycerol 1-palmitate	37.509	0.50	C ₁₉ H ₃₈ O ₄
15	Docosanoic acid, methyl ester	37.893	0.74	C ₂₃ H ₄₆ O ₂
16	Tetracosanoic acid, methyl ester	40.967	0.59	C ₂₅ H ₅₀ O ₂

TABLE 9. FAME CONTENT IN PALM STEARIN BIODIESEL

FAME type	Compound name	Chemical formula	Content (%)
Saturated FAME	Octanoic acid, methyl ester	C ₉ H ₁₈ O ₂	0.29
	Decanoic acid, methyl ester	C ₁₁ H ₂₂ O ₂	0.29
	Dodecanoic acid, methyl ester	C ₁₃ H ₂₆ O ₂	3.60
	Methyl tetradecanoate	C ₁₅ H ₃₀ O ₂	11.16
	Hexadecanoic acid, methyl ester	C ₁₇ H ₃₄ O ₂	24.79
	Heptadecanoic acid, methyl ester	C ₁₈ H ₃₆ O ₂	1.34
	Methyl stearate	C ₁₉ H ₃₈ O ₂	13.20
	Eicosanoic acid, methyl ester	C ₂₀ H ₄₀ O ₂	4.39
	Docosanoic acid, methyl ester	C ₂₃ H ₄₆ O ₂	0.74
	Tetracosanoic acid, methyl ester	C ₂₅ H ₅₀ O ₂	0.59
	Total saturated FAME		
Unsaturated FAME	Methyl hexadec-9-enoate	C ₁₇ H ₃₂ O ₂	1.19
	9,12-Octadecadienoic acid (Z, Z)-, methyl ester	C ₁₉ H ₃₄ O ₂	13.64
	9-Octadecenoic acid (Z)-, methyl ester	C ₁₉ H ₃₆ O ₂	21.90
	cis-Methyl 11-eicosenoate	C ₂₀ H ₃₈ O ₂	1.74
Total unsaturated FAME			38.47
Total FAME			97.66

the environment. Biodiesel's physicochemical properties, such as viscosity, oxidative stability, cold flow properties, cetane number, energy content, lubricity and biodegradability, significantly depend on the proportion of FAME it contains. To maximise these qualities and ensure that biodiesel is suitable for various applications, such as power production, heating and transportation, it is imperative to balance the concentrations of saturated and unsaturated FAME (Brahma *et al.*, 2022).

CONCLUSION

This study effectively optimised the transesterification process for the production of biodiesel from palm stearin using a Box-Behnken design and RSM. We created a quadratic model to clarify the interactions between methanol volume, catalyst quantity, and reaction time. With a coefficient of determination (R^2) of 0.9849 and an Adj- R^2 of 0.9974, the model shows a great match to the experimental data, demonstrating its excellent predictive accuracy. Further evidence of the model's importance in maximising biodiesel output comes from the low p -value (<0.0001). The ideal parameters of 225 mL of methanol, 10 g of catalyst and a 60-min reaction period resulted in a maximum biodiesel output of 910 mL, with a percentage yield of 89.25%. We validated the model's effectiveness by finding that the expected biodiesel production nearly matches the experimental result. Physicochemical studies revealed that the produced biodiesel exhibited good viscosity, density and cold flow characteristics. These characteristics are essential for guaranteeing both environmental sustainability and optimal engine performance. While this study offers valuable insights, future research should explore scaling up the process for industrial applications to assess the practical feasibility of these optimised conditions at a larger scale. The study's limitations include the laboratory-scale nature of the experiments. Further studies could address potential variations in yield or biodiesel quality under different operational scales and raw materials, which would provide a more comprehensive understanding of the process's broader applicability.

ACKNOWLEDGEMENT

The authors would like to thank the IITM SAIF (Sophisticated Analytical Instrument Facility) for their vital role in delivering the GC-MS data required for the biodiesel sample analysis and characterisation.

REFERENCES

- Adepoju, T., Victor, E., Ekop, E., Emberru, R., Balogun, T., & Adeniyi, A. (2022). Residual wood ash powder: A predecessor for the synthesis of CaO-K₂O-SiO₂ base catalyst employed for the production of biodiesel from *Asimina triloba* oil seed. *Case Studies in Chemical and Environmental Engineering*, 6, 100252. <https://doi.org/10.1016/j.cscee.2022.100252>
- Bai, H., Tian, J., Talifu, D., Okitsu, K., & Abulizi, A. (2022). Process optimisation of esterification for deacidification in waste cooking oil: RSM approach and for biodiesel production assisted with ultrasonic and solvent. *Fuel*, 318, 123697. <https://doi.org/10.1016/j.fuel.2022.123697>
- Brahma, S., Nath, B., Basumatary, B., Das, B., Saikia, P., Patir, K., & Basumatary, S. (2022). Biodiesel production from mixed oils: A sustainable approach towards industrial biofuel production. *Chemical Engineering Journal Advances*, 10, 100284. <https://doi.org/10.1016/j.cej.2022.100284>
- Buasri, A., Lertnimit, S., Nisapruksachart, A., Khunkha, I., & Loryuenyong, V. (2023). Box-Behnken design for optimization on esterification of free fatty acids in waste cooking oil using modified smectite clay catalyst. *ASEAN Journal of Chemical Engineering*, 23(1), 40–51. <https://doi.org/10.22146/ajche.77009>
- Buasri, A., Kamsuwan, J., Dokput, J., Buakao, P., Horthong, P., & Loryuenyong, V. (2024). Green synthesis of metal oxides (CaO-K₂O) catalyst using golden apple snail shell and cultivated banana peel for production of biofuel from non-edible *Jatropha curcas* oil (JCO) via a central composite design (CCD). *Journal of Saudi Chemical Society*, 101836. <https://doi.org/10.1016/j.jscs.2024.101836>
- Bustamam, F. K. A., Yeoh, C. B., Sulaiman, N., & Saw, M. H. (2022). Evaluation on the quality of Malaysian refined palm stearin. *OCL*, 29, 37. <https://doi.org/10.1051/ocl/2022030>
- Danane, F., Bessah, R., Alloune, R., Tebouche, L., Madjene, F., Kheirani, A. Y., & Bouabibsa, R. (2022). Experimental optimisation of waste cooking oil ethanolysis for biodiesel production using response surface methodology (RSM). *Science and Technology for Energy Transition*, 77, 14. <https://doi.org/10.2516/stet/2022014>
- Deivajothi, P., Manieniyar, V., & Sivaprakasam, S. (2018). An impact of ethyl esters of groundnut

- acid oil (vegetable oil refinery waste) used as emerging fuel in DI diesel engine. *Alexandria Engineering Journal*, 57(4), 2215–2223. <https://doi.org/10.1016/j.aej.2017.09.003>
- DieselNet. (2024). *Biodiesel standards & properties*. Retrieved January 30, 2024, from https://dieselnet.com/tech/fuel_biodiesel_std.php
- Gupta, S., Patel, P., & Mondal, P. (2022). Biofuels production from pine needles via pyrolysis: Process parameters modeling and optimisation through combined RSM and ANN-based approach. *Fuel*, 310, 122230. <https://doi.org/10.1016/j.fuel.2021.122230>
- Hazrat, M. A., Rasul, M. G., Mofijur, M., Khan, M. M. K., Djavanroodi, F., Azad, A. K., Bhuiya, M. M. K., & Silitonga, A. S. (2020). A mini review on the cold flow properties of biodiesel and its blends. *Frontiers in Energy Research*, 8. <https://doi.org/10.3389/fenrg.2020.598651>
- Hussanai, S., & Kittisak, W. (2023). Optimisation of FAME production from waste cooking palm oil with KOH catalyst supported on palm kernel shells ash (PKSA) using response surface methodology (RSM). *Journal of Oil Palm Research*, 35(4), 668–681. <https://doi.org/10.21894/jopr.2023.0005>
- Joorasty, M., Rahbar-Kelishami, A., & Hemmati, A. (2022). A performance comparison of cyclopentyl methyl ether (CPME) and hexane solvents in oil extraction from sewage sludge for biodiesel production; RSM optimisation. *Journal of Molecular Liquids*, 368, 120573. <https://doi.org/10.1016/j.molliq.2022.120573>
- Karimi, S., & Saidi, M. (2022). Biodiesel production from *Azadirachta indica*-derived oil by electrolysis technique: Process optimisation using response surface methodology (RSM). *Fuel Processing Technology*, 234, 107337. <https://doi.org/10.1016/j.fuproc.2022.107337>
- Khan, T. A., Khan, T. A., & Kumar Yadav, A. (2022). A hydrodynamic cavitation-assisted system for optimisation of biodiesel production from green microalgae oil using a genetic algorithm and response surface methodology approach. *Environmental Science and Pollution Research*, 29(32), 49465–49477. <https://doi.org/10.1007/s11356-022-20474-w>
- Kober, R., Schwaab, M., Barbosa-Coutinho, E., & Pinto, J. C. (2022). Are empirical models based on the response surface methodology suitable for biodiesel production optimisation? *Industrial & Engineering Chemistry Research*, 61(34), 12458–12472. <https://doi.org/10.1021/acs.iecr.2c01848>
- Loryuenyong, V., Rohing, S., Singhanam, P., Kamkang, H., & Buasri, A. (2024). Artificial neural network and response surface methodology for predicting and maximizing biodiesel production from waste oil with KI/CaO/Al₂O₃ catalyst in a fixed bed reactor. *ChemPlusChem*, 89. <https://doi.org/10.1002/cplu.202400117>
- Manimaran, R., Venkatesan, M., & Kumar, K. T. (2022). Optimisation of okra (*Abelmoschus esculentus*) biodiesel production using RSM technique coupled with GA: Addressing its performance and emission characteristics. *Journal of Cleaner Production*, 380, 134870. <https://doi.org/10.1016/j.jclepro.2022.134870>
- Manojkumar, N., Muthukumaran, C., & Sharmila, G. (2022). A comprehensive review on the application of response surface methodology for optimisation of biodiesel production using different oil sources. *Journal of King Saud University-Engineering Sciences*, 34(3), 198–208. <https://doi.org/10.1016/j.jksues.2020.09.012>
- Muthuswamy, S., & Veerasigamani, M. (2020). Impact of secondary fuel injector in various distances on direct injection diesel engine using acetylene-biodiesel in reactivity controlled compression ignition mode. *Energy Sources, Part A: Recovery, Utilization, and Environmental Effects*, 1–15. <https://doi.org/10.1080/15567036.2020.1810177>
- Ngige, G. A., Ovuoraye, P. E., Igwegbe, C. A., Fetahi, E., Okeke, J. A., Yakubu, A. D., & Onyechi, P. C. (2023). RSM optimisation and yield prediction for biodiesel produced from alkali-catalytic transesterification of pawpaw seed extract: Thermodynamics, kinetics, and multiple linear regression analysis. *Digital Chemical Engineering*, 6, 100066. <https://doi.org/10.1016/j.dche.2022.100066>
- Parak, S., Nikseresht, A., Alikarami, M., & Ghasemi, S. (2022). RSM optimisation of biodiesel production by a novel composite of Fe (III)-based MOF and phosphomolybdic acid. *Research on Chemical Intermediates*, 48(9), 3773–3793. <https://doi.org/10.1007/s11164-022-04783-w>
- Rajali, N. A., Radzi, S. M., Rehan, M. M., & Amin, N. A. M. (2022). Optimisation of the biodiesel production via transesterification reaction of palm oil using response surface methodology

- (RSM): A review. *Malaysian Journal of Science, Health & Technology*, 8(2), 58–67. <https://doi.org/10.33102/mjosht.v8i2.292>
- Ranjan, A., Dawn, S. S., Nirmala, N., Santhosh, A., & Arun, J. (2022). Application of deep eutectic solvent in biodiesel reaction: RSM optimisation, CI engine test, cost analysis and research dynamics. *Fuel*, 307, 121933. <https://doi.org/10.1016/j.fuel.2021.121933>
- Razak, N. H., Hashim, H., Yunus, N. A., & Klemeš, J. J. (2021). Reducing diesel exhaust emissions by optimisation of alcohol oxygenates blend with diesel/biodiesel. *Journal of Cleaner Production*, 316, 128090. <https://doi.org/10.1016/j.jclepro.2021.128090>
- Sakkampang, C., Sakkampang, K., Suwunnasopha, P., & Poojeera, S. (2023). Performance, exhaust emission, and wear behavior of a direct-injection engine using biodiesel from Yang-Na (*Dipterocarpus alatus*) oleoresins. *Case Studies in Chemical and Environmental Engineering*, 7, 100328. <https://doi.org/10.1016/j.csee.2023.100328>
- Sakthivel, R., Ramesh, K., Purnachandran, R., & Mohamed Shameer, P. (2018). A review on the properties, performance, and emission aspects of the third generation biodiesels. *Renewable and Sustainable Energy Reviews*, 82, 2970–2992. <https://doi.org/10.1016/j.rser.2017.10.037>
- Simsek, S., Uslu, S., & Simsek, H. (2022). Proportional impact prediction model of animal waste fat-derived biodiesel by ANN and RSM technique for diesel engine. *Energy*, 239, 122389. <https://doi.org/10.1016/j.energy.2021.122389>
- Sonachalam, M., PaulPandian, P., & Manieniyar, V. (2020). Emission reduction in diesel engine with acetylene gas and biodiesel using inlet manifold injection. *Clean Technologies and Environmental Policy*, 22, 2177–2191. <https://doi.org/10.1007/s10098-020-01968-y>
- Theam, K. L., Islam, A., Choo, Y. M., & Taufiq-Yap, Y. H. (2015). Biodiesel from low cost palm stearin using metal doped methoxide solid catalyst. *Industrial Crops and Products*, 76, 281–289. <https://doi.org/10.1016/j.indcrop.2015.06.058>
- Verma, P., & Sharma, M. P. (2016). Comparative analysis of effect of methanol and ethanol on Karanja biodiesel production and its optimisation. *Fuel*, 180, 164–174. <https://doi.org/10.1016/j.fuel.2016.04.035>
- Vyas, A. P., Verma, J. L., & Subrahmanyam, N. (2011). Effects of molar ratio, alkali catalyst concentration, and temperature on transesterification of jatropha oil with methanol under ultrasonic irradiation. *Advances in Chemical Engineering and Science*, 1(2), 45–50. <https://doi.org/10.4236/aces.2011.12008>
- Yusoff, M. N. A. M., Zulkifli, N. W. M., Sukiman, N. L., Kalam, M. A., Masjuki, H. H., Syahir, A. Z., Awang, M. S. N., Mujtaba, M. A., Milano, J., & Shamsuddin, A. H. (2022). Microwave irradiation-assisted transesterification of ternary oil mixture of waste cooking oil – *Jatropha curcas*-palm oil: Optimization and characterization. *Alexandria Engineering Journal*, 61(12), 9569–9582. <https://doi.org/10.1016/j.aej.2022.03.040>
- Zahan, K. A., & Kano, M. (2018). Biodiesel production from palm oil, its by-products, and mill effluent: A review. *Energies (Basel)*, 11(8), 2132. <https://doi.org/10.3390/en11082132>
- Zhang, C., Chang, J., Wang, T., & Lu, C. (2019). Biodiesel production from waste cooking oil using a novel heterogeneous catalyst derived from hydrotalcite-supported KOH. *Fuel*, 236, 1016–1024. <https://doi.org/10.3934/energy.2022049>